

1 Towards agricultural soil carbon monitoring, reporting and 2 verification through Field Observatory Network (FiON)

3 Olli Nevalainen¹, Olli Niemitalo², Istem Fer¹, Antti Juntunen², Tuomas Mattila³, Olli Koskela², Joni
4 Kukkamäki², Layla Höckerstedt¹, Laura Mäkelä⁴, Pieta Jarva⁴, Laura Heimsch¹, Henriikka Vekuri¹, Liisa
5 Kulmala^{1,5}, Åsa Stam¹, Otto Kuusela^{1,6,7}, Stephanie Gerin¹, Toni Viskari¹, Julius Vira¹, Jari Hyväluoma²,
6 Juha-Pekka Tuovinen¹, Annalea Lohila^{1,6}, Tuomas Laurila¹, Jussi Heinonsalo⁵, Tuula Aalto¹, Iivari
7 Kunttu², Jari Liski¹

8

9 ¹ Finnish Meteorological Institute, FMI, Helsinki, Finland

10 ² Häme University of Applied Sciences, HAMK, Hämeenlinna, Finland

11 ³ Finnish Environment Institute, SYKE, Helsinki, Finland

12 ⁴ Baltic Sea Action Group, BSAG, Espoo, Finland

13 ⁵ University of Helsinki, Institute for atmospheric and Earth system research (INAR), forest sciences, Helsinki, Finland

14 ⁶ University of Helsinki, Institute for atmospheric and Earth system research (INAR), physics, Helsinki, Finland

15 ⁷ University of Amsterdam, Computational Science, Amsterdam, Netherlands

16

17 *Correspondence to:* (olli.nevalainen@fmi.fi)

18 **Abstract.** Better monitoring, reporting and verification (MRV) of the amount, additionality and persistence of the sequestered
19 soil carbon is needed to understand the best carbon farming practices for different soils and climate conditions, as well as their
20 actual climate benefits or cost-efficiency in mitigating greenhouse gas emissions. This paper presents our Field Observatory
21 Network (FiON) of researchers, farmers, companies and other stakeholders developing carbon farming practices. FiON has
22 established a unified methodology towards monitoring and forecasting agricultural carbon sequestration by combining offline
23 and near real-time field measurements, weather data, satellite imagery, modeling and computing networks. FiON's first phase
24 consists of two intensive research sites and 20 voluntary pilot farms testing carbon farming practices in Finland. To disseminate
25 the data, FiON built a web-based dashboard called Field Observatory (v1.0, fieldobservatory.org). Field Observatory is
26 designed as an online service for near real-time model-data synthesis, forecasting and decision support for the farmers who are
27 able to monitor the effects of carbon farming practices. The most advanced features of the Field Observatory are visible on the
28 Qvidja site which acts as a prototype for the most recent implementations. Overall, FiON aims to create new knowledge on
29 agricultural soil carbon sequestration and effects of carbon farming practices, and provide an MRV tool for decision-support.

30

31 **1 Introduction**

32 Farmers are managing one of the largest carbon stocks on the planet where even relatively small additions are important for
33 climate change mitigation. Accordingly, the international “soil carbon 4 per mille” initiative aims at raising the soil organic
34 carbon content by 0.4 % per year by adopting carbon farming practices (Minasny et al. 2017). Carbon farming practices include
35 methods, such as increasing carbon inputs (soil amendments, cover crops, residue management) and crop rotations. Such
36 practices do not only have the potential to partially refill the global soil carbon stock that has lost 116 Pg carbon due to land
37 cultivation (Sanderman et al., 2017), but they could also improve soil structure and health, and increase crop yields (Merante
38 et al. 2017; Oldfield et al. 2018). Annual carbon sequestration rates for different management practices vary from 100 to 1000
39 kg C ha⁻¹ (Merante et al., 2017; Minasny et al., 2017). Detecting sequestration rates in this range is difficult with traditional
40 empirical soil sampling designs due to large spatial variability of soil carbon content and small relative changes in the soil
41 carbon stock due to individual management actions (VandenBygaart and Angers 2006; Heikkinen et al. 2021). This calls for
42 better monitoring, reporting and verification (MRV) of the amount, additionality and persistence of the sequestered soil carbon
43 due to carbon farming practices.

44
45 Towards this goal, we established the Field Observatory Network (FiON), a network of researchers, farmers, companies and
46 other stakeholders applying carbon farming practices. FiON has created a unified methodology to monitor and forecast
47 agricultural carbon sequestration, by combining automated near real-time field measurements, weather data, satellite imagery,
48 modeling and computing networks. In general, FiON follows the principles of other ecological observatory networks, such as
49 National Ecological Observatory Network (NEON, Keller et al., 2008), Global Lake Ecological Observatory Network
50 (GLEON, Hipsey et al., 2017) and Biodiversity Observatory Networks (GEOBON, Guerra et al., 2021) that collect long-term
51 ecological data and monitor the effects of climate and land use change (Elmendorf 2016; Hinckley et al., 2016; Hipsey et al.,
52 2017; Keller et al., 2008). The primary purpose of FiON, however, is to i) create new knowledge on soil processes, ii) to
53 measure, verify and forecast the carbon sequestration in agricultural soils and to iii) approximate the effects of carbon farming
54 practices on yield, biomass and CO₂ flux in near real-time. To achieve this, FiON invested in the use and development of a
55 community cyberinfrastructure tool, Predictive Ecosystem Analyzer (PEcAn, pecanproject.org), which enables synthesizing
56 different data sources and process-based models, quantifying and partitioning uncertainties, and operationalizing near real-
57 time ecological forecasting (Fer et al., 2021). To disseminate the observations and findings, we built a free-access online
58 dashboard called Field Observatory (v1.0, fieldobservatory.org). This website serves as a tool to monitor the impacts of carbon
59 farming practices. The dashboard integrates data from field sensors, remote sensing and field survey. In this sense, FiON will
60 provide decision support for the farmers, at first hand via the Field Observatory website and in due course via the scientific
61 synthesis informed by the best available data and models. To serve the research and other interested communities, the data in
62 Field Observatory is publicly available and downloadable from the website.

63

64 In this paper our objectives are to 1) describe data flows from various manual and automatic measurements in the Field
65 observatory, 2) demonstrate 15-day forecasts of carbon exchange and plant growth towards decision support for the farmers,
66 and 3) discuss the benefits of the public monitoring network established by FiON.

67

68 First, we introduce the sites included in FiON, and describe the tested carbon farming practices. Next, we describe the FiON
69 workflow from data collection, processing and storage to visualization and dissemination through the Field Observatory
70 website. Finally, we present the near real-time model-data synthesis, forecasting and decision support for the users.

71 **2 Sites and tested carbon farming practices**

72 The first phase of FiON consists of two intensive agricultural research sites and 20 voluntary farms testing carbon farming
73 practices (Fig. 1, <https://www.fieldobservatory.org/MapView>). These 20 farms, called Advanced Carbon Action farms (ACA),
74 were selected out of 100 pilot farms participating in the Carbon Action platform¹, where volunteer farmers test carbon farming
75 practices (Mattila et al. 2022). Each farm has a test field and an adjacent, conventionally managed, control field (field 1 and 0
76 in Field Observatory, respectively). The additional carbon farming practices aim to increase carbon stock through increasing
77 carbon inputs (photosynthesis & soil amendments) or through decreasing carbon decomposition (Minasny et al., 2017). These
78 practices (Table 1) are: cover crops, adaptive grazing, soil amendments, subsoiling and ley farming (introducing a grass crop
79 into rotation). Each farmer made a five-year carbon farming plan and took soil samples at the beginning of the study from GPS
80 located points in the field. The same points are monitored annually and also contain real-time soil sensors.

81

1

Carbon Action platform consists of several scientific projects, 100 farms committed to 5 years of research activity and farmer extension services. As of spring 2021, some 600 farmers are participating around the topic. Food system companies and organisations are also involved. Carbon Action is led by BSAG and the research is coordinated by FMI. More <https://carbonaction.org/en/front-page/>

82

83

Table 1 Principles of the carbon farming practices tested at the Carbon Action farms.

Carbon farming practice	Principles for carbon sequestration
Cover crops	Crops planted to lengthen photosynthetically active period and to increase carbon inputs from above and belowground biomass and to reduce leaching of carbon and nutrients.
Adaptive grazing	Short grazing & long rest periods to manage grass growth for increased root growth and increased soil cover.
Soil amendments	Exogenous carbon input. High input of organic material may stimulate plant growth through increased water holding capacity, nutrients, etc.
Subsoiling	Removing physical barriers to root growth by soil loosening. Coupled to a grass crop to stabilize loosened soil. Increases plant growth and soil aeration and decreases bulk density.
Ley farming	Breaking monocropping with perennial grass. Increases photosynthesis, root input and diversity.
Grass cultivation	Diverse plant species composition, increased cutting height and organic fertilization.

84

85

86

87

88

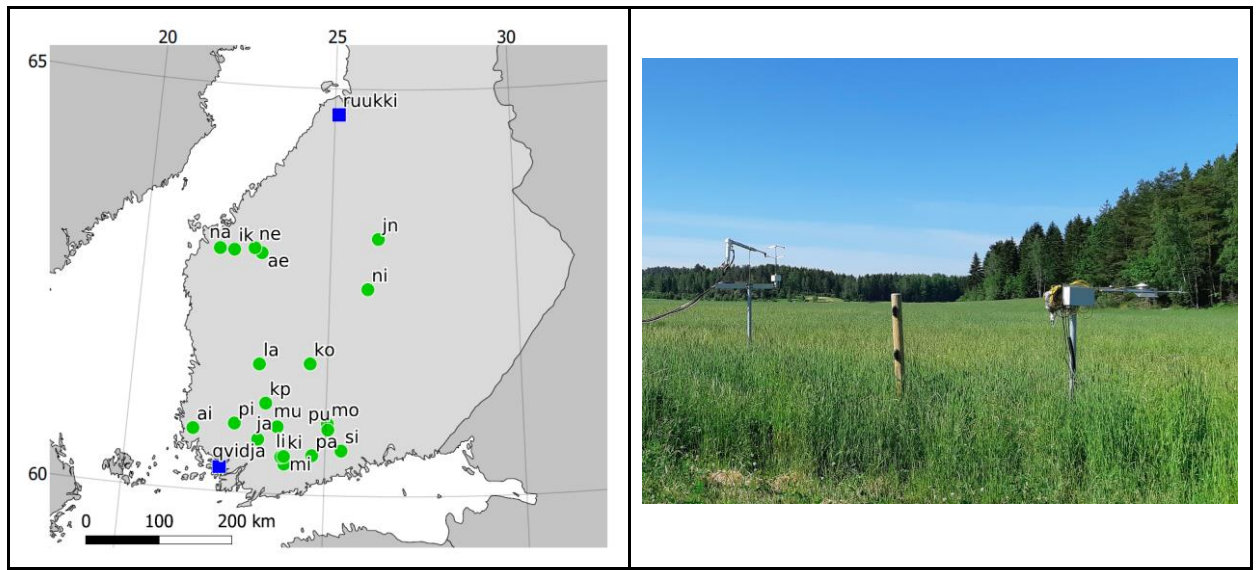
89

90

91

92

The 20 ACA farms were selected based on their chosen practice (four farms per measure), location (appropriate distances for survey work and even spread over Finnish farmland) and soil type (a mix of clay and sandy soils) (Table 2). All of them were included in a soil quality survey in 2019 (Mattila, 2020). Farms with anomalous measurements or too large organic matter content or nutrient differences between the control and treatment plots in the initial phase of FiON were excluded from ACA farms. FiON includes two intensive research sites, Qvidja and Ruukki, which are operated by the Finnish Meteorological Institute (FMI). In Qvidja, carbon farming practices are tested in three different fields. In Ruukki, there are no carbon farming practices implemented at the moment. Both sites have eddy covariance towers which continuously monitor greenhouse gas fluxes and weather (see Sect. 3).



93

94 **Figure 1** Map of Advanced Carbon Action sites (green dots) and intensive sites (blue squares) (left), and eddy covariance
 95 tower and radiation measurement instrumentation at Qvidja (right).

96

97 **Table 2** Current FiON sites.

Site	Site type	Soil type	Carbon farming practice	Species in 2020	Nearest FMI weather station
AE	ACA	Sandy loam	Subsoiling	Rye	Kauhava airport
KO	ACA	Silt	Subsoiling	Silage grass	Juupajoki Hyytiälä
KP	ACA	Clay loam	Subsoiling	Multi-species ley	Pirkkala airport
LA	ACA	Clay silt	Subsoiling	Oats	Pirkkala airport
JN	ACA	Fine sand	Adaptive grazing	Pasture grass	Vesanto Sonkari
MI	ACA	Clay loam	Adaptive grazing	Pasture grass	Lohja Porla
NI	ACA	Sand till	Adaptive grazing	Pasture grass	Jyväskylä airport AWOS
KI	ACA	Fine sand	Soil amendments	Multi-species ley	Somero Salkola
LI	ACA	Clay loam	Soil amendments	Spring wheat	Lohja Porla
PA	ACA	Clay loam	Soil amendments	Hay grass	Nurmijärvi Röykkä
PI	ACA	Clay loam	Soil amendments	Oats	Kaarina Yltöinen

MU	ACA	Clay loam	Grass mixture	Multi-species ley	Somero Salkola
NA	ACA	Loam	Cover crops	Peas	Vaasa airport
NE	ACA	Loam	Cover crops	Oats	Kauhava airport
PU	ACA	Silty clay loam	Cover crops	Oats	Mäntsälä Hirvihaara
SI	ACA	Clay loam	Cover crops	Multi-species ley	Porvoo Harabacka
AI	ACA	Silty clay	Ley farming	Multi-species ley	Rauma Pyynpää
JA	ACA	Clay loam	Ley farming	Multi-species ley	Jokioinen Ilmala
IK	ACA	Sand till	Ley farming	Silage grass	Seinäjäki Pelmaa
MO	ACA	Loam	Ley farming	Barley	Hämeenlinna Lammi Pappila
Qvidja	Intensive	Clay loam	Grass cultivation	Silage grass	Kaarina Yltöinen*
Ruukki	Intensive	Organic (peat)	-	Silage grass	Siikajoki Ruukki*

98 *Intensive sites have their own micrometeorological measurements.

99

100 **3 Data collection**

101 FiON combines multiple online and offline data streams with different temporal frequencies and geographical extent (Fig. 2,
102 Table 3). These data streams flow into a server where the data are pre-processed (filtered, gap-filled, formatted) and model-
103 data analyses are performed through an ecological cyberinfrastructure Predictive Ecosystem Analyzer (PEcAn, Fer et al.,
104 2021). All observational and computational outputs are stored in the server and disseminated through a web-based user
105 interface. In the following sections we describe each data stream and model-data activity in the order given in Fig. 2.

106

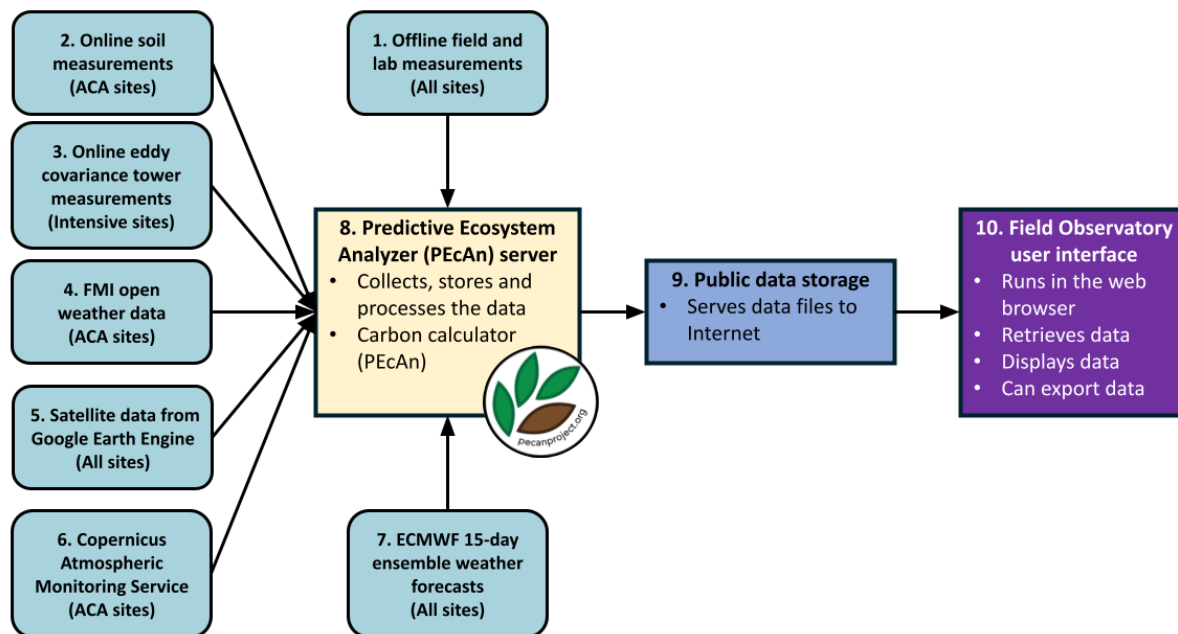


Figure 2 Overview of the FiON data flows.

3.1 Offline field and lab measurements

At ACA sites, the measurements are done at three georeferenced points per field. The points have c.a. 30–100 m distance from each other and are located on a transect line. The transect was situated on each field to ensure comparable conditions for both the test and control plots. When placing the transects, slope, vegetation map and soil type were used to ensure the transect covers different management zones in the field. Annual soil sampling and soil quality measurements are made within a ten-meter radius of these points. All offline data from ACA sites on soil properties (cation exchange capacity, pH, organic matter), nutrients (P, K, S, Ca, Mg, Cu, Zn, B, Mn, Fe, Al, P-saturation), soil physical quality (soil structure, bulk density, porosity, water holding capacity, infiltration rate) and biological properties (earthworm counts, above ground biomass, percentage plant cover) are presented in Zenodo data repository with annual updates (Mattila, 2020; Mattila and Heinonen, 2021). In addition to annual monitoring, a pre-study SOC sampling was conducted on the fields in 2018 and will be repeated in 2023. In these studies, ten 20 cm deep core soil samples (14 mm diameter) were collected at 10 m radius from a georeferenced point centre and pooled to form a composite sample. Such samples were taken from each field from the three measurement points from both the control and carbon farming fields. Focusing the sampling to georeferenced locations and using composite sampling,

123 reduces the overall sampling variability and allows tracking relatively small (4 % of background level) changes in SOC stock
124 (Knebl et al. 2015). The offline field measurements at the intensive site Qvidja are described in Heimsch et al. (2021).

125 Offline, non-automated and infrequent data are currently being curated further for harmonization and reporting in JavaScript
126 Object Notation (JSON) file formats and International Consortium for Agricultural Systems Applications (ICASA) standards
127 (White et al., 2013). An example soil carbon measurement data point ($16.59 \pm 2.25 \text{ kg m}^{-2}$, average \pm standard deviation) is
128 visualized on Qvidja graphs and available on the accompanying JSON file ([https://data.lit.fmi.fi/field-](https://data.lit.fmi.fi/field-observatory/qvidja/ec/events.json)
129 [observatory/qvidja/ec/events.json](https://data.lit.fmi.fi/field-observatory/qvidja/ec/events.json)).

130 **3.1.1 Field activity**

131 All field activity information (e.g. planting, fertilization, harvest timing and amount) is currently received offline through
132 personal communication. An online application is under development for i) harmonizing historical field data, and for ii)
133 collecting future field activity data. Accordingly, the application is being developed to allow the farmers themselves to enter
134 these events and related details, and it will be tested for the first time at the end of the 2021 season. The application is written
135 using the Shiny R package (v1.6.0, Chang et al., 2021) and it automatically produces files in a JSON format using the ICASA
136 standards when possible (https://github.com/Ottis1/fo_management_data_input). Examples of historical field activity events
137 (e.g. planting and tillage) that are prepared through this application are being made available in the Field Observatory JSON
138 files and visualized on the graphs (Fig. 5).

139 **3.2 Online soil measurements**

140 Since 2020, each ACA site was provided with four TEROS-12 soil sensors (METER Group, Inc. USA) (two sensors per field,
141 control and treatment) measuring volumetric water content, electrical conductivity and temperature (Table 3). The automated
142 sensors are located at 75 mm depth in two of the three fixed measurement points of each field. The sensors were connected to
143 a third party data transfer hardware (Datasense Oy, Finland), which uses Lora/WAN network to transmit the data. During the
144 first year, the sensors measured every half hour but in 2021 measurement frequency was changed to one hour. The data is
145 stored at the service providers server and is pulled to the PEcAn server (#8) through the Datasense API. Currently the sensor
146 array includes 80 TEROS-12 soil sensors, four O₂ sensors (Apogee Instruments, SO-120, USA) and two CO₂ sensors (Vaisala
147 Oy, G525, Finland) and will be supplemented with weather and groundwater depth measurements. The soil O₂ and CO₂ meters
148 are used to track changes in soil microbial activity and to guide model development.

149 **3.3 Online eddy covariance measurements**

150 Carbon dioxide, evapotranspiration (latent heat), sensible heat and momentum fluxes between the ecosystem and atmosphere
151 are measured at the intensive study sites, Ruukki and Qvidja, using the micrometeorological eddy covariance (EC) technique.
152 The EC instrumentation at both sites includes a three-axis sonic anemometer (uSonic-2 Scientific, METEK GmbH, Elmshorn,

153 Germany) and an enclosed-path infrared gas analyser (LI-7200, LI-COR Biosciences, NE, USA) installed on a tower. The
154 measurement height is 2.3 m in Qvidja and 3.3 m in Ruukki (2.3 m from 13 June to 25 June 2019, 3.1 m from 25 June to 4
155 November 2019 and 3.3 m since 5 November 2019). The measurement heights fulfill guidelines for grasslands and croplands
156 defined by the Integrated Carbon Observation System (ICOS; Sabbatini & Papale, 2017). For details of the measurement set-
157 up in Qvidja, see Heimsch et al. (2021).

158 The data from the EC instruments are recorded at a 10-Hz frequency. Half-hourly turbulent fluxes are calculated by block-
159 averaging these raw data after applying a double rotation of the coordinate system (McMillen, 1988). The time lag between
160 the sonic anemometer and gas analyzer signals is determined based on the cross-correlation analysis (Rebmann et al., 2012).
161 The gas fluxes are calculated from the mixing ratios determined with respect to dry air (Webb et al., 1980). The measured
162 fluxes are compensated for the losses due to high-frequency signal attenuation within the measurement system (Laurila et al.,
163 2005). The flux data are filtered for instrument malfunction and unfavourable flow conditions according to the following
164 generic validity criteria: number of spikes in the raw data < 100, mean CO₂ mixing ratio > 350 ppm, relative stationarity (Foken
165 and Wichura, 1996) < 30 % and CO₂ mixing ratio variance < 15 ppm² from April to September and < 5 ppm² from October to
166 March. At the Ruukki site, flux data are accepted from the wind direction sector 135°-315° (Blocks 5, 6, 5up and 6up) and the
167 sectors 0°-90° and 330°-360° (Blocks 1-4). In Qvidja, the wind directions representing the direction of the experimental site
168 are 0°-30° and 140°-360°. Periods of weak turbulence are filtered by applying a site-specific friction velocity threshold. The
169 threshold and its uncertainty are estimated for each site-year using the moving-point-transition method (Reichstein et al., 2005)
170 and a bootstrapping approach (Pastorello et al., 2020). For incomplete years, the estimates from the previous year are used.
171 While the flux data provided online are screened, they will be subject to further quality control in offline post-processing that
172 will produce the final datasets distributed for scientific use. These post-processing procedures include flux footprint analysis
173 and related data screening for inadequate upwind fetch, i.e., for cases in which the measured flux does not predominantly
174 represent the field. Footprints are calculated with respect to the effective measurement height that takes into account the varying
175 canopy height and snow depth.

176 The EC measurements are complemented with supporting meteorological observations conducted next to the flux tower. These
177 include soil moisture, soil temperature at different depths, soil heat flux, photosynthetically active radiation (PAR), global and
178 reflected solar radiation, air temperature and precipitation. Half-hourly meteorological and flux data are transmitted to a server
179 at the FMI, which is then synchronized to the PEcAn server (#8).

180 **3.3.1 Flux gap-filling and uncertainty analysis**

181 The missing CO₂ flux (net ecosystem exchange, NEE) data are gap-filled based on empirical response functions that are fitted
182 separately for the gross primary production (GPP) and total ecosystem respiration (ER):

$$183 \quad NEE = GPP + ER \quad (1)$$

184 Respiration is modelled as a function of air temperature:

$$185 \quad ER = R_0 \cdot e^{E_0 \cdot \left(\frac{1}{T_0} - \frac{1}{T_a - T_1} \right)} \quad (2)$$

186 where R_0 is the respiration rate at the reference temperature of 283.15 K, $T_0 = 227.13$ K, $T_1 = 56.02$ K, E_0 is the temperature
187 sensitivity of respiration, and T_a is the measured air temperature (Lloyd and Taylor, 1994).

188 GPP is modelled as a function of PAR:

$$189 \quad GPP = \frac{\alpha \cdot PAR \cdot GP_{max}}{\alpha \cdot PAR + GP_{max}} \quad (3)$$

190 where α is the apparent quantum yield and GP_{max} is the asymptotic photosynthesis rate in optimal light conditions.

191 For gap-filling, the data are divided into sections based on the harvest dates, and each section is gap-filled separately. This is
192 done because fluxes measured before a harvest cannot be used to predict fluxes after a harvest. First, R_0 and E_0 are estimated
193 from the night-time ($PAR < 20 \mu\text{mol m}^{-2} \text{s}^{-1}$) flux data with a 15-day moving window. If there are less than 25 observations,
194 the window size is increased stepwise by two days until enough data are obtained. Similarly, α and GP_{max} are determined with
195 a three-day moving window by fitting the PAR response function to the daytime NEE from which the modelled respiration is
196 subtracted. Finally, gaps in NEE are filled with modelled NEE, which is the sum of modelled GPP and modelled ER. Gap-
197 filled values that are determined using fits from asymmetrical time windows, with possibly biased data are flagged and updated
198 when new measurements become available. Before flux gap-filling, the missing air temperature and PAR data are imputed
199 using linear interpolation if the gap is not longer than 6 h. Longer gaps are filled using the mean diel cycle of the data measured
200 within seven days before or after the missing data point

201 The uncertainty of measured NEE (u_{meas}) is inferred from the model residuals. For each site-year, the measurements are
202 grouped into $0.2 \text{ mg CO}_2 \text{ m}^{-2} \text{ s}^{-1}$ wide bins, and for each bin the measurement uncertainty is characterized as the standard
203 deviation of the residuals. The uncertainty of each measured half-hourly flux is then estimated from the relation between the
204 measurement uncertainty and the magnitude of the flux (Richardson et al., 2008). For incomplete years, the relation from the
205 previous year is used.

206 The uncertainty of modelled NEE (u_{mod}), Eqs. (1)–(3), is propagated from the uncertainties of the least-squares fits of modelled
207 GPP (u_{GPP}) and Reco (u_{Reco}) as:

$$208 \quad u_{mod} = \sqrt{u_{GPP}^2 + u_{Reco}^2} \quad (4)$$

209 Finally, the uncertainty related to the friction velocity threshold (u_{ustar}) is estimated by filtering the flux data using the 100
210 different bootstrapped friction velocity thresholds, gap-filling the 100 differently filtered datasets, and using the standard
211 deviation of the gap-filled fluxes as an estimate for u_{ustar} .

212 **3.4 FMI open weather data**

213 For all ACA sites, the weather information, namely precipitation, air temperature, relative humidity, wind speed and wind
214 direction are retrieved from the nearest FMI weather stations (Table 2). Weather data are pulled to the PEcAn server using the
215 fmir R package (<https://github.com/mikmart/fmir>).

216 **3.5 Satellite data from Google Earth Engine (GEE)**

217 All sites are monitored using remote sensing imagery from European Space Agency's (ESA) Sentinel-2 satellites.
218 Atmospherically corrected Level-2A (L2A) Sentinel-2 multispectral data (processed using Sen2Cor software) are retrieved
219 using GEE (earthengine.google.com) cloud data platform. The scene classification band available in L2A products is used to
220 filter away image acquisition dates during which the field is covered by snow, cloud or cloud shadow. From the Sentinel-2
221 data, we calculate the Normalized Difference Vegetation Index (NDVI) and the Leaf Area Index (LAI). LAI is calculated
222 because it is present in and can be assimilated to many process-based ecosystem models. NDVI is included in Field
223 Observatory mainly for the farmers to whom NDVI is a more familiar measure compared to LAI. NDVI is calculated using
224 near infra-red (B8A) and red (B4) bands of the L2A products. LAI is estimated using the ESA Sentinel Application Platform
225 (SNAP) Biophysical Processor neural network algorithm (Weiss & Baret, 2016,
226 <https://github.com/ollinevalainen/satellitertools>). The NDVI data is natively available in 10 m resolution, whereas LAI is
227 resampled to 10 m resolution from its original 20 m resolution. The satellite data is updated every two days at most (which is
228 the Sentinel-2 revisit frequency over Finland). In addition, yearly cumulative NDVI sum is calculated using integration by
229 trapezoidal rule for all sites ("NDVI days"). Common starting and ending points for the active growing season, 31 March and
230 31 October, respectively, are used to standardize the cumulative NDVI sums between sites. This standardization improves the
231 comparability of the cumulative sums between sites by having them all in the same absolute units. Without standardization the
232 cumulative sums would be much influenced by the availability of the first and last observations of the growing season for a
233 site. This is determined more by the cloud cover than the actual start and end of the growing season. To improve within site
234 comparison, the cumulative NDVI is computed using dates when all fields within a site have satellite imagery available. The
235 NDVI and LAI data is provided to the Field Observatory user interface in both raster (GeoTIFF) and tabular form (CSV).

236 With the tabular data, the average value of pixels within the field is used to estimate the field-level value. The tabular data is
237 provided with 90 % confidence intervals by multiplying the associated uncertainties by the Z-score for two-sided 90 %
238 confidence interval (1.645). Non-realistic negative LAI values are capped to zero. For NDVI the uncertainty is presented as
239 standard error of the mean (SE) of the pixels within the field. For the cumulative NDVI sum, the uncertainties are propagated

240 using the Python uncertainties package (<https://pythonhosted.org/uncertainties/>) which automatically computes the required
241 derivatives and propagates the uncertainties.

242 The uncertainty for the LAI (u_{LAI}) is estimated by combining the observational uncertainty (SE_{LAI}) and the algorithmic
243 uncertainty (u_{alg}) of the LAI estimation:

$$244 \quad u_{LAI} = \sqrt{SE_{LAI}^2 + u_{alg}^2}, \quad (5)$$

245 where the SE_{LAI} is computed as the SE of LAI observations within the field. The observational uncertainty aims at capturing
246 the uncertainty associated with a particular single observation (from a specific image at a certain date). It is affected by the
247 variability of the individual pixel values within the field at that specific date. The u_{alg} is calculated by propagating theoretical
248 individual pixel uncertainties (u_{t_i}) to the calculated average:

$$249 \quad u_{alg} = n^{-1} \sqrt{\sum_{i=1}^n u_{t_i}^2}, \quad (6)$$

250 where n is the number of pixels (i.e. sample size) and u_t the reported theoretical RMSE for the SNAP LAI algorithm that is
251 0.89 (Weiss and Baret, 2016) and constant to all pixels. The artificial increase of n due to resampling LAI observations from
252 its native 20 m resolution to 10 m is taken into account and n is reduced accordingly.

253 **3.6 PAR from Copernicus Atmospheric Monitoring Service (CAMS)**

254 For the ACA sites, the daily PAR data are derived from the global irradiation data obtained from the CAMS through daily
255 queries (www.soda-pro.com/web-services/radiation/cams-radiation-service/, Qu et al., 2017). The global daily irradiation (Wh
256 $\text{m}^{-2} \text{day}^{-1}$) is converted to daily PAR ($\text{MJ m}^{-2} \text{day}^{-1}$) assuming that 50 % of the global irradiation is at PAR range. The CAMS
257 data is available for each day with a 48 h time lag. The daily PAR is reported in $\text{MJ m}^{-2} \text{day}^{-1}$ which is a more convenient unit
258 for a daily value compared to $\mu\text{mol m}^{-2} \text{s}^{-1}$ used with 30-min measurement frequency in intensive sites.

259 **3.7 ECMWF 15-day ensemble weather forecasts**

260 European Center Medium-range Weather Forecast (ECMWF) data are processed by the Finnish Meteorological Institute for
261 every site. This dataset consists of 6-hourly 2 meter temperature ($2t$ variable in ECMWF standards), total precipitation (tp),
262 relative humidity (r), 10 meter U and V wind components ($10u$ and $10v$, respectively), surface pressure (sp), surface solar and
263 thermal radiation downwards ($ssrd$ and $strd$, respectively) values of 51 ensemble members where one member is the control
264 forecast and the other 50 are perturbed members which have perturbed initial conditions different than the control to explore

265 the range of uncertainty (Buizza and Richardson, 2017). Weather forecast data are updated everyday. Per ECMWF license
 266 agreements, the data are visualized as is but the disseminated tabular files are obfuscated.

267 **Table 3 Summary of data streams reported in FiON. Offline = stored in public data repository and updated as necessary.**

Data type	Units	Data source	Frequency	Since	Sites	Online/offline
Field activity	-	Personal communication*	Seasonal	2019	All	Offline
Farmer management actions	-	Questionnaire	Annual		All	Offline
Soil C	% (ACA), kg m ⁻² (Qvidja)	Lab measurements	Biannual	2018	All, except Ruukki	Offline
Soil water holding capacity	m ³ m ⁻³	Lab measurements	Once to calibrate sensors	2019	All, except Ruukki	Offline
Soil nutrients	mg kg ⁻¹	Lab measurements	Biannual	2018	ACA	Offline
Bulk density	kg dm ⁻³	Lab measurements	Annual	2019	ACA	Offline
Biomass	kg ha ⁻¹	Lab measurements	Annual	2019	ACA	Offline
Soil moisture	m ³ m ⁻³	ACA soil sensors & eddy covariance	Half-hourly	2018 (Qvidja), 2019 (Ruukki), 2020 (ACA)	ACA & Intensive	Online
Soil temperature	°C	ACA soil sensors & eddy covariance	Half-hourly	2018 (Qvidja), 2019 (Ruukki), 2020 (ACA)	ACA & Intensive	Online
Electrical conductivity	μS cm ⁻¹	ACA soil sensors	Half-hourly	2020	ACA	Online
CO ₂ -flux	mg m ⁻² s ⁻¹	Eddy covariance	Half-hourly	2018 (Qvidja), 2019 (Ruukki)	Intensive	Online
Latent and sensible heat flux	W m ⁻²	Eddy covariance	Half-hourly	2018 (Qvidja), 2019 (Ruukki)	Intensive	Online
Short-wave radiation (incoming and reflected)	W m ⁻²	Eddy covariance	Half-hourly	2018 (Qvidja), 2019 (Ruukki)	Intensive	Online
CO ₂ concentration	ppm	Eddy covariance	Half-hourly	2018 (Qvidja), 2019 (Ruukki)	Intensive	Online
Precipitation	mm	FMI open weather & eddy covariance	Half-hourly	2018 (Qvidja), 2019 (ACA & Ruukki)	ACA & Intensive	Online

Air Temperature	°C	FMI open weather & eddy covariance	Half-hourly	2018 (Qvidja), 2019 (ACA & Ruukki)	ACA & Intensive	Online
Relative Humidity	%	FMI open weather & eddy covariance	Half-hourly	2018 (Qvidja), 2019 (ACA & Ruukki)	ACA & Intensive	Online
PAR	MJ m ⁻² day ⁻¹ μmol m ⁻² s ⁻¹	Copernicus & eddy covariance	Daily & half-hourly	2018 (Qvidja), 2019 (ACA & Ruukki)	ACA & Intensive	Online
Leaf Area Index	m ² m ⁻²	Sentinel-2, GEE	Min 2-days	2018 (Qvidja), 2019 (ACA & Ruukki)	All	Online
NDVI	-	Sentinel-2, GEE	Min 2-days	2018 (Qvidja), 2019 (ACA & Ruukki)	All	Online

268 *Online application is under development.

269 **3.8 Predictive Ecosystem Analyzer (PEcAn) server**

270 All FiON data are pooled in an FMI server where model-data integration cyberinfrastructure software PEcAn is installed and
271 compiled. PEcAn is an ecological informatics toolbox that consists of process-based models, a workflow management system
272 and analytical tools for model-data synthesis (LeBauer et al., 2013; Dietze et al., 2013). The automated PEcAn workflow calls
273 a series of modularized tasks that involve pre-processing of the model inputs, configuring and running the models, post-
274 processing model outputs and performing model-data integration analyses. Coupling a process-based model to this workflow
275 requires writing a model package which consists of a few interfacing scripts as PEcAn adopts intermediate input and output
276 file formats, and applies pre- and post-model run analyses to these standards (Fer et al., 2021). While there are already many
277 ecosystem models coupled to PEcAn and its design is general across process-based models, coupling of more models that can
278 simulate agricultural ecosystems is in progress. In this study, we coupled the BASGRA_N model (Basic Grassland Model,
279 Höglind et al., 2020) to the PEcAn workflow and demonstrated its use for the Qvidja site (see Sect. 4, Model-data synthesis).
280 In the future, we will provide model predictions for all sites through PEcAn.

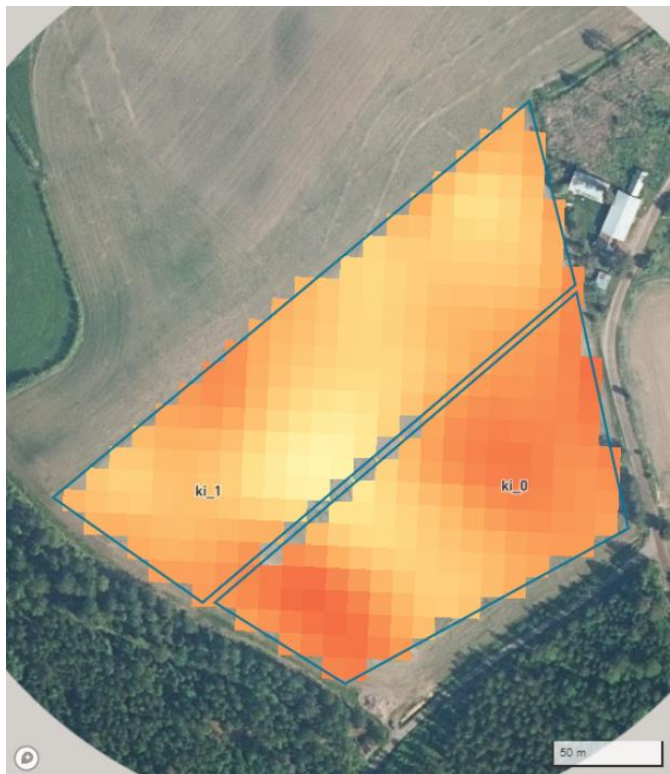
281 **3.9 Public data storage**

282 To harmonize the data, all tabular data with less than daily measurement frequency is aggregated to a 30 min interval (to every
283 hour and half hour) before transferring the data to the public data storage (Amazon Simple Storage Service, field-
284 observatory.data.lit.fmi.fi). To protect the privacy of the farmers, all data holding spatial information is transformed for all
285 ACA sites, except for site MU (which is operated by Häme University of Applied Sciences).

286 **3.10 Field Observatory user interface**

287 The Field Observatory user interface (v1.0, fieldobservatory.org) allows viewing general information about the sites and the
288 measurements and carbon farming practices conducted on them. The website has an interactive map to navigate to site-specific
289 dashboards. A site view consists of general information about the site, an interactive map with satellite imagery of a specified
290 vegetation parameter, an interactive timeline for selecting satellite imagery for viewing, and a panel of interactive time series
291 charts (Fig. 3). Each chart comes with a description of the displayed data. A chart typically contains multiple time series and
292 the visibility of each can be toggled. The user can enable and disable time aggregation and choose the time aggregation level
293 from predefined options. The time aggregation is calculated using sliding statistics such as mean or sum depending on the data
294 type. Any chart can be exported as an SVG image or as a CSV file containing the displayed data. A global specification file
295 defines a list of charts and the data source types that can be shown in each chart. Site-specific specification files are used to
296 define data source types available for each site and to provide links to the data files. Specification files are stored in JSON
297 format.

298 The website is served by Azure services. The map and site views are based on client-side JavaScript, running in the user's web
299 browser. Maps have been implemented using Mapbox GL JS JavaScript library.



KI

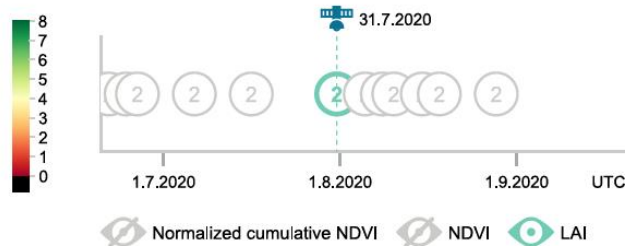
Advanced CarbonAction Site

KI field is a low OM sand in organic crop rotation. The aim is to increase OM by adding organic matter through soil amendments (wood pulp, ramial woodchips).

FARMING METHODS

Management: soil amendments
Species: multi-species ley
Soil type: fine sand

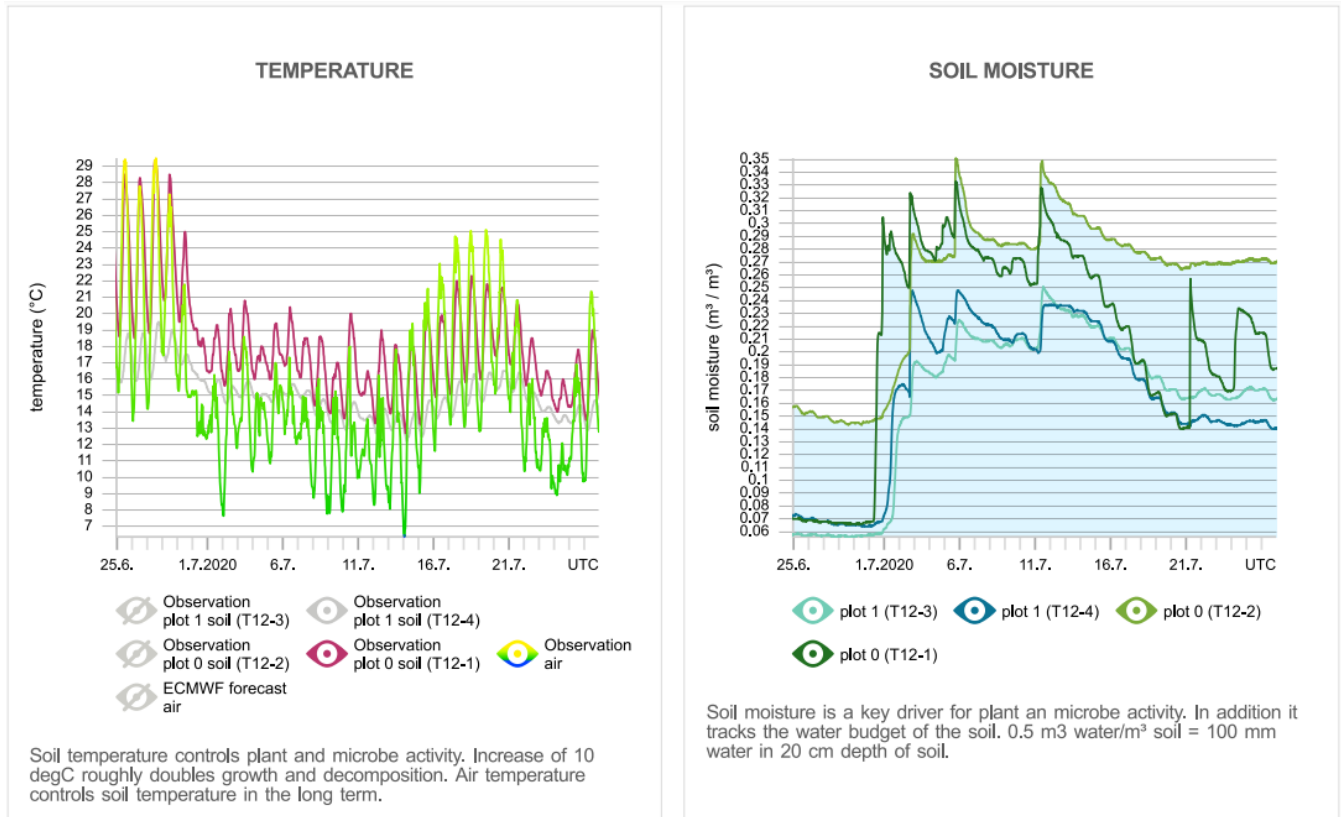
SATELLITE IMAGES



300

301
302
303

(a)



304

305

(b)

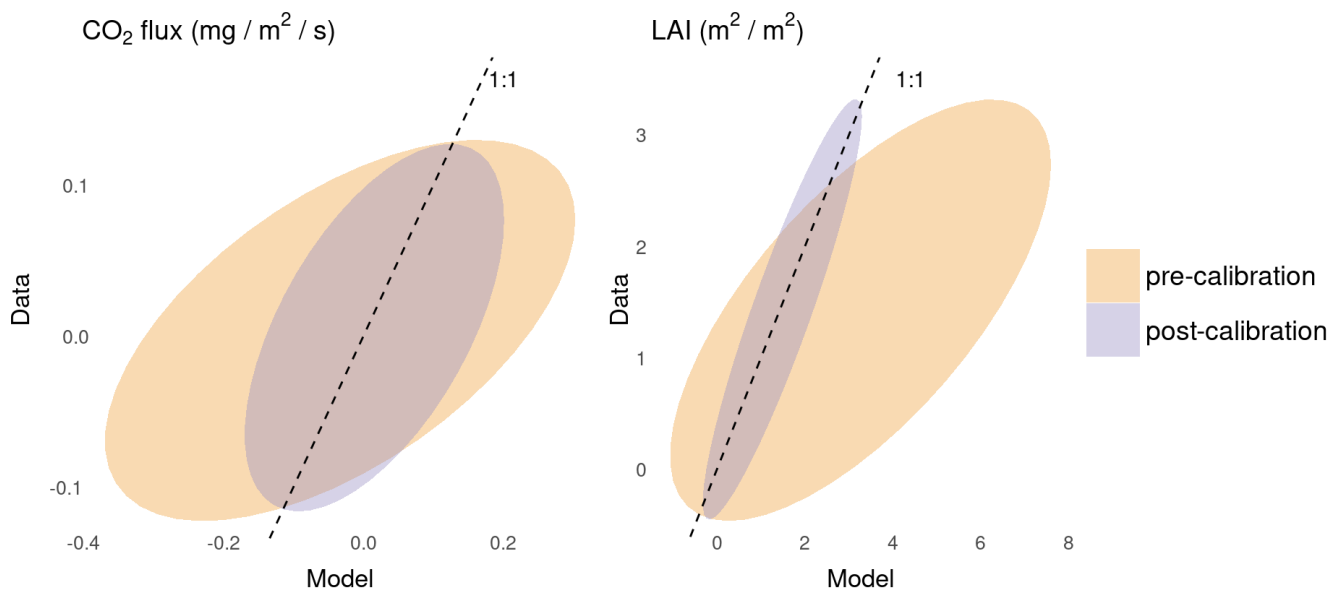
306 **Figure 3** Two web interface views of the measurement data for site KI: (a) Overview and LAI satellite images and (b) observed
307 soil and air temperature and soil moisture. The reader is referred to the website www.fieldobservatory.org for more and
308 interactive charts. The aerial photo contains data from the National Land Survey of Finland Topographic Database (11/2020).

309 **4 Model-data synthesis and decision support**

310 While the current version of the Field Observatory mainly disseminates observations, one of the main goals of this application
311 is to provide accessible near real-time model-data synthesis, forecasting and decision support for the users. We demonstrate

312 the first application of this service at the Quidja grassland site with the grassland model BASGRA_N (Table 2). BASGRA_N
313 model is developed specifically for northern climates and for grass types (timothy, *Phleum pratense*; meadow fescue, *Festuca*
314 *pratensis*) that are the dominating forage species cultivated at the Quidja farm, and it is able to simulate grassland productivity,
315 quality and greenhouse gas balance (Höglind et al., 2020).

316
317 We coupled BASGRA_N to PEcAn, and used PEcAn's workflow management system and analytical tools (specifically the
318 Bayesian calibration and state data assimilation modules) to inform the model with the data. Before employing them for
319 forecasting and decision support, these models need to be initialized and calibrated. In other words, while state data assimilation
320 algorithms can inform model states and improve predictive performance, best results are achieved when the model is calibrated
321 to the site (Huang et al., 2021). Therefore, we used the field and lab measurements (Sect. 3.1), such as the rooting depth, soil
322 carbon content and soil water holding capacity, to initialize the model states. Next, using multiple constraints (CO₂ flux and
323 LAI from the eddy covariance tower field, Sect. 3.3), we calibrated 20 model parameters using Bayesian numerical methods
324 through the BayesianTools R-package (Hartig et al., 2019) as implemented in the PEcAn system (Fer et al., 2018, also please
325 see the supplement, section S1 for further details on the calibration protocol). In calibration, we used the observations from
326 May 2018 to April 2021. After calibration model predictions were improved in terms of both uncertainty reduction and
327 accuracy (Fig. 4). While the model is calibrated by the EC field data at Quidja, initial results show improvement at the nearby
328 Quidja ACA sites as well (not shown here, but visible on Field Observatory LAI graphs).

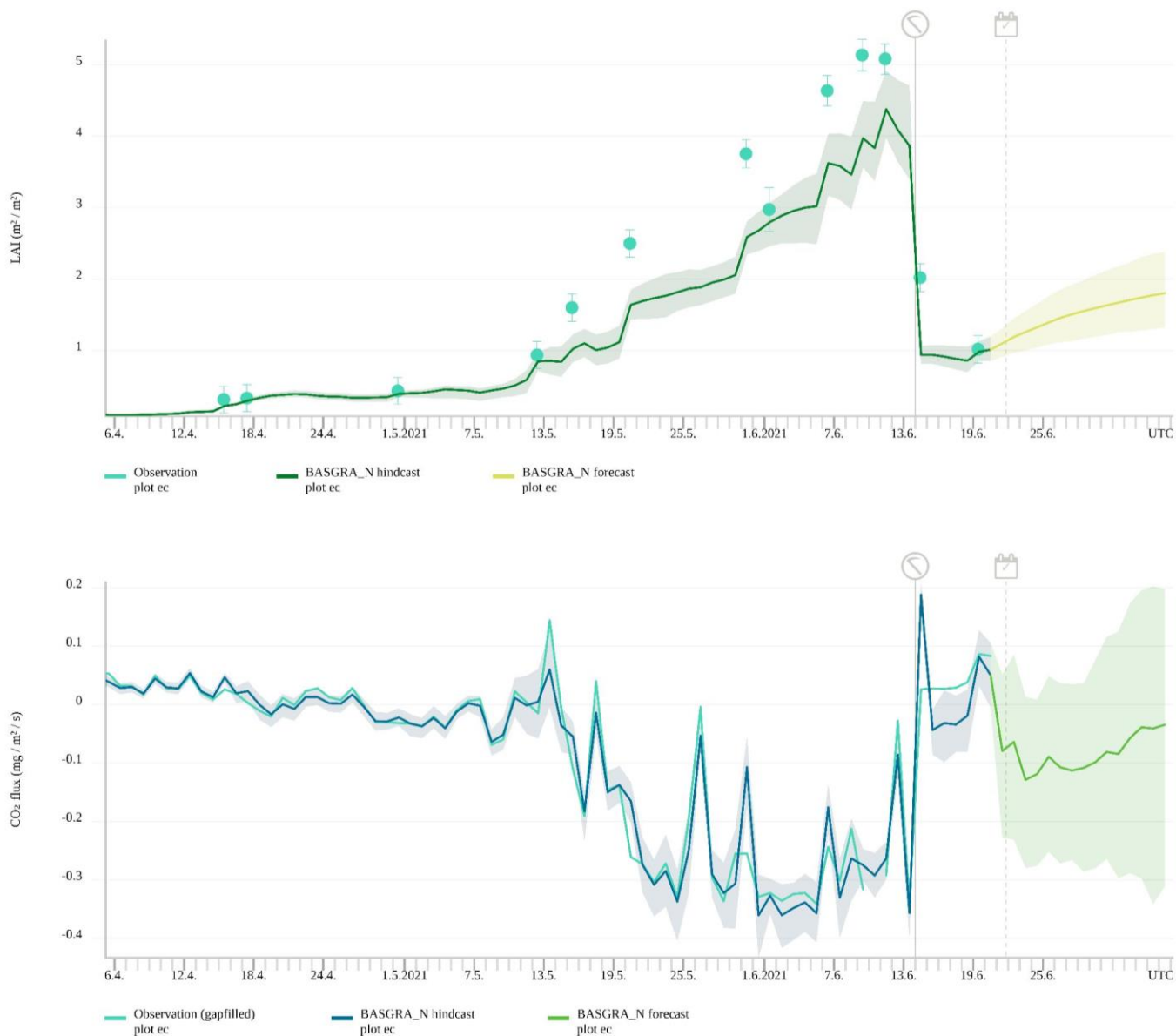


329
330
331 **Figure 4** Predicted versus observed comparison before (orange ellipses) and after (purple ellipses) initialization and
332 calibration. Ellipses represent the 90 % confidence intervals of model ensemble runs with 500 members. After initialization

333 and calibration, the model performance at Quidja improved in terms of both accuracy (closer to the 1:1 line) and uncertainty
334 reduction (narrower ellipses).

335

336 Next, we deployed the initialized and calibrated model in an online, operational, iterative near-term forecasting framework by
337 driving it with the ECMWF ensemble 15-day weather forecast (Sect. 3.7). From April 2021 onwards, every day a 15-day
338 ensemble forecast is made from the BASGRA_N model. As time progresses, each day the CO₂ flux forecast is informed with
339 the observed and gap-filled daily CO₂ flux values within an iterative forecast-analysis cycle using the Ensemble Adjustment
340 Kalman filter algorithm implemented in PEcAn (Dietze, 2017). When LAI observations are also available, they are jointly
341 assimilated with the CO₂ flux measurements as well. Although we are currently only assimilating the CO₂ flux and LAI
342 observations, related states are also updated within the model through the analysis step as the model encodes and simulates
343 relations and covariances among different ecosystem processes. Among the model output variables, we share the LAI and CO₂
344 flux (Fig. 5), as well as Latent Heat and Yield Potential forecasts with the users through the Field Observatory user interface,
345 albeit only for the Quidja site for the time being.



346

347 **Figure 5** 15-day LAI (top) and CO₂ flux (bottom) forecast at Qvidja. The 90 % confidence intervals for hindcast and forecast
 348 are generated by 250 ensemble members, with different combinations of model parameters, initial conditions and
 349 meteorological drivers. Units in the CO₂ flux graph are given per second to reflect the measurement frequency, however,
 350 observations were aggregated to daily time step here to align with the model predictions. The scythe icon indicates a harvest
 351 event on June 14th, 2021.

352

353 While a 15-day forecast has limited applicability within a cropping cycle, it could be informative on certain field activities that
354 may have 1–2 weeks of flexibility which in return may have an impact on carbon balance. For instance, one can simulate
355 alternative scenarios of timing of the harvest (e.g. whether to harvest now or delay it, please see supplementary material S2
356 for a demonstration). It is possible to retrospectively explore these cases systematically as both weather forecasts and model
357 analysis states are archived in the Field Observatory’s operational iterative forecasting system.

358 **5 Discussion**

359 This paper introduced the Field Observatory Network (FiON) and its unified methodology leading the way to monitor and
360 forecast the functioning of agricultural ecosystems, geared towards verification of soil carbon sequestration. This methodology
361 combines the existing spatially scattered measurements, modeling and computing networks, and disseminates the model-data
362 computation outcomes through the Field Observatory user interface. In the following, we discuss the scientific and practical
363 contributions of FiON and the Field Observatory, and the future steps planned for both.

364 **5.1 Scientific contribution**

365 FiON adopts state-of-the-art field and laboratory methods, open data sources, near real-time satellite imagery processing and
366 model-data integration cyberinfrastructures—all of which are needed for a reliable MRV platform. A distinct feature of FiON
367 is the network of ordinary farms, ACA sites, to establish baseline trends and verify additional changes. As soil carbon pool
368 changes slowly, even after a shift in management practices, long-term monitoring is needed. The ACA sites (with control and
369 treatment plots) were specifically designed for this purpose and will be monitored continuously for at least the next five years,
370 and FiON aspires to continue even longer. This is an adequate time frame to detect SOC changes because the fastest carbon
371 re-accumulation occurs in the first 10–20 years, depending on soil type, management practices, climate and initial SOC (Bossio
372 et al., 2020), all of which are monitored by FiON. The intensive and ACA sites provide an important benchmarking opportunity
373 to our model-data synthesis methodology which will be applied to all 100 Carbon Action farms.

374
375 The PEcAn platform is central to our methodology; it enables synthesizing different data sources and process-based models,
376 managing observational and model uncertainties, and near real-time forecasting. It distinguishes FiON from observations-only
377 approaches. In addition to potentially having practical relevance for improving carbon storage, near-term agricultural
378 forecasting has benefits to basic carbon science. Data assimilation methods help dissect model behaviour and identify research
379 needs (Viskari et al., 2020). For instance, variability patterns of the best parameter sets in time and space can be identified by
380 studying model ensemble members with respect to the analysis states (i.e. our best understanding about the system) and may
381 point to unaccounted processes in models and underlying sources driving variability. If we manage to account for these
382 variabilities (e.g. adding covariates that explain temporal variability), we could also improve our capability to model the carbon
383 sequestration on the long term. Moreover, near-term iterative forecasting provides an out-of-sample way of statistical testing

384 for models which is less prone to overfitting than in-sample tests which are more typical in (agro-)ecology where models are
385 tested against data that has already been observed (Dietze et al., 2018). Accordingly, a more in-depth analysis of the archived
386 Field Observatory forecasting results and skills are ongoing and will be reported in a future study. In addition to understanding
387 models better, operational iterative near-term forecasting also allows us to detect and intervene when measurements of certain
388 sensors or data streams deviate from the assimilated background, and in return supports the management of the sensors and
389 data pipelines, resulting in higher quality datasets. Overall, our 15-day iterative forecasting system provides continuous
390 quantitative benchmarking of models and data based on all other available information, which allows rapid detection and
391 explanation of changing patterns in the carbon sequestration with the possibility of intervening and making adjustments.

392 **5.2 Practical contribution**

393 The Field Observatory user interface has not only enabled farmers to monitor impacts of their carbon farming practices, but
394 also to connect and compare their own and others' data and practices. Features in the user interface are co-created with the
395 farmers and developed accordingly. For example, farmers requested to see a cumulative sum of NDVI through the growing
396 season which was in return calculated and included on the website. Likewise, simple and clear descriptions to interpret each
397 data type have been found helpful. The gap-filled CO₂ fluxes at the intensive study sites have made it easier to communicate
398 carbon exchanges between land and the atmosphere and how carbon budget calculations are done. As a result, the Field
399 Observatory has already been used in workshops and meetings with stakeholders, and in training and scientific outreach for
400 the Carbon Action farmers.

401
402 One of our aims with this framework is to provide decision support for the end users. This is effectively offered by Field
403 Observatory in terms of feedback where end users can monitor the impact of their activities in a quantitative manner, assess
404 and make their decisions in the future accordingly. Our framework also lays the groundwork for a more explicit and specific
405 decision support system. Although such functionality is not fully in place yet (but under development), establishing the
406 operational data assimilation and iterative forecasting pipeline is a milestone towards this direction. While the 15 days' horizon
407 has limitations with respect to the span of a production cycle, in the future we are planning to include seasonal, annual and
408 longer term forecasts as well. However, 15-day forecasts can still provide decision support for relatively shorter term and
409 flexible agricultural actions (such as harvest, irrigation, grazing etc.). With the additional layer of agricultural forecast on top
410 of the weather forecasting services, users are quantitatively informed about the progression of various ecosystem states and
411 services through these Field Observatory near-term forecast updates. For example, sensor or model-based dynamic fertilization
412 strategies have successfully improved the nitrogen use efficiency of cropping systems (e.g. Sela et al., 2018; Scharf et al.,
413 2011). Likewise, timing of harvest and the cutting height may affect the overall carbon budget and economic income, and the
414 plants' water demand may necessitate a different irrigation scheme for optimum growth and water usage, all of which may not
415 readily manifest themselves through weather forecasts and observations only. We also acknowledge that such interventions

416 are potentially easier for grasslands, as opposed to the croplands. Nevertheless, our operative iterative near-term forecasting
417 system enables a framework to explore the impacts of such interventions dynamically, systematically and quantitatively, and
418 in return devise more reliable and comprehensive decision criteria. Overall, the current pipeline is being developed to improve
419 the model performance and to be put into an adaptive decision making framework where alternative scenarios will be simulated
420 with the models to aid users in their day-to-day operations specific to their management structure and goals.

421
422 The near-term carbon forecasts have also improved our communication with stakeholders in general. Reporting quantitative,
423 specific and iterative carbon forecasts makes it possible to convey the idea that predictive carbon science has the potential to
424 be as successful and common as numerical weather prediction (NWP) as a discipline and as a service to society one day.
425 Ecological forecasts provide us with a standard, quantitative, intuitive and management-relevant method and language to
426 develop the right context and tools for structuring soil carbon sequestration decisions (Petchey et al., 2015; Dietze et al., 2018).
427 Bringing near-term carbon forecasts forward further helps describe that soil carbon monitoring and modeling is a complex
428 computational problem that depends on vast amounts of basic scientific research and observations. It involves a diverse range
429 of actors and organizations and requires efficient communication and continuous transfer of knowledge between these groups,
430 similar to NWP (Bauer et al., 2015). Not only the similarities but also the differences between agricultural forecasting and
431 NWP help clarify and re-focus the research needs (e.g. the need to address the heterogeneity and inherent variability in carbon
432 systems). Overall, near-term forecasts help establish this constructive dynamic between researchers and stakeholders which in
433 return helps tackle remaining bottlenecks for improving soil carbon sequestration more efficiently.

434
435 There is a large interest towards adopting and developing Field Observatory further. Therefore, the website is under constant
436 development with new features, and new information about carbon farming and findings of FiON are increasingly being made
437 available.

438 **5.3 Avenues for future research and development**

439 We have planned future steps for both FiON and the Field Observatory. The first step is to add more agricultural models to
440 PEcAn. This enables us to extend model-data analysis to all FiON sites where different species and management practices are
441 involved (i.e. other than grass harvest timing and amount). Coupling of one such additional model (Simulateur
442 multIdisciplinaire pour les Cultures Standard, STICS, Brisson et al., 1998) to PEcAn has already been completed, and others
443 are in progress. In the meantime, more sites will be added to FiON, not only in number but also in type. For example, with
444 carbon-smart planning, urban vegetation also has potential to store more carbon. We study this also in FiON and consequently
445 urban sites will be added. Another goal is to include forests and peatlands in FiON, which requires incorporating new process-
446 based models in the FiON workflow. During the coming years, more field and laboratory measurement data will be collected
447 and used to validate the model estimates and re-calibrate the models.

448

449 The framework designed by FiON and described in this paper provides the necessary mechanics to study the applicability and
450 reliability of the models to simulate components of the carbon budget virtually in every field. While scalability has been the
451 core idea for the design of this framework since the beginning, putting it to practical test is the main scientific next step.
452 Currently, a factorial experimental design and simulation is ongoing where the performance of the models will be tested at
453 multiple sites by informing them with various data streams. For this, we will start with constraints that can be made available
454 virtually from everywhere and test which combinations, if any, can inform models enough to capture local carbon budget
455 dynamics and components. Such constraints are for example LAI derived from remote sensing, soil moisture provided by
456 inexpensive in-situ sensors, soil properties estimated from global products and yield. In this setup, the information contributed
457 by the sites that are equipped with EC-towers will also be tested. For example, we will perform a factorial experiment at the
458 ACA sites with and without the models being constrained by EC-data at the intensive sites. As we have additional data streams
459 other than the mentioned constraint data types (e.g. biomass and soil C, Table 2) from ACA sites for evaluation, the framework
460 described in this paper provides the means to carry out such multi-site in-depth analyses.

461
462 The development of the online application to gather field activity data from farmers is also in progress. The main purpose of
463 this application is to make collection and utilization of field activity data in visualization and model-data synthesis pipelines
464 easy. In this context, Field Observatory's interoperability with commercial farm management information systems needs to be
465 studied in order to reduce the number of times farmers are filling out such information. An additional future use of this online
466 application is planned to enable the farmers to simulate a predefined number of scenarios regarding their day-to-day operations
467 by triggering automated PEcAn workflows—for example, given the next 15-day forecast, they will be able to optimize the
468 timing and amounts of their field activity. We are also considering utilizing this online application for additional purposes: a)
469 for compiling information from farmers regarding the flexibilities of their activities as this brings an additional practical
470 constraint on the development of the model-based decision support system, b) for enabling new users to submit electronic
471 requests and information about their fields to be part of the FiON network, c) for supporting peer-to-peer learning between
472 farmers (Mattila et al., 2022).

473
474 We are currently also investigating the use of satellite data sources other than Sentinel-2 in retrieving information on vegetation
475 and soil properties. In addition to satellite imagery, drones could be used as a source of remote sensing data. The current
476 Sentinel-2 data filtering is based on the cloud detection available in the L2A products. This filtering approach has produced
477 quite clean time series; some sites do not have any outliers and some have at the maximum one or two per year. The benefit
478 of our methodology—where we assimilate observations as state variables to process-based models—is that single outliers,
479 with optimally larger uncertainties, do not have too drastic of an effect on the model predictions. Nevertheless, we will continue
480 to follow the performance of the filtering approach and improve it if necessary. Finally, the data streams used in data
481 assimilation (to inform and update forecasts) will be increased and improvement in forecasting skills will be analyzed.

482 **6 Conclusions**

483 The Field Observatory Network (FiON) introduced in this paper is primarily a network of researchers, farmers, companies and
484 other stakeholders developing carbon farming practices. FiON provides a unified methodology to monitor and forecast
485 agricultural carbon sequestration by combining offline and near real-time field measurements, weather data, satellite imagery,
486 modeling and computing networks. FiON disseminates data through the Field Observatory user interface
487 (www.fieldobservatory.org). For farmers, FiON serves as a monitoring and decision support tool. In contrast to the mainstream
488 decision support tools, FiON also provides the farmers access to other carbon farmers' data in the network. This enables
489 comparisons and knowledge transfer between the carbon farmers.

490 FiON has several analogies to other ecological observatory networks, but unlike these existing networks, FiON is designed to
491 provide near real-time information and forecasts concerning the carbon farming practices and to facilitate monitoring and
492 verification of carbon sequestration. In this sense, FiON takes several steps forward from the mainstream of the ecological
493 observatory networks known so far.

494 **7 Data availability**

495 The data displayed in the Field Observatory are available from the Field Observatory website (www.fieldobservatory.org) and
496 from Amazon Simple Storage Service at <https://field-observatory.data.lit.fmi.fi/index.html>. Field measurements conducted at
497 ACA sites in 2019 and 2020 are available from Zenodo data repository (Mattila, 2020; Mattila and Heinonen, 2021).

498 **8 Code availability**

499 The satellite data processing codes are available from a public GitHub repository
500 (<https://github.com/ollinevalainen/satellitertools>). All PEcAn code is available openly on a GitHub repository
501 (<https://github.com/PecanProject/pecan>). Field Activity data collection and curation application code which is under
502 development is also available via GitHub (https://github.com/Ottis1/fo_management_data_input). Rest of the codes by the
503 authors are not yet openly available.

504

505 **9 Author contribution**

506 Conceptualization, ON, ONi, IF, AJ, TM, OK, JK, LH, LM, PJ, LK, ÅS, AL, JHe, IK, JL; Data curation, ON, IF, ONi, TM,
507 OKu; Formal Analysis, ON, IF, ONi, TM, LHe, HV, SG, TV, JV, JT, Funding acquisition, TM, LK, AL, TL, JHe, TA, IK, JL;
508 Investigation, ON, IF, ONi, TM, LHe, HV, SG, TV, JV, JT; Methodology, ON, IF, ONi, TM, HV, LK, OKu, TV, JV, JT, JHe,

509 TA, JL; Project administration, TM, JK, LH, LK, ÅS, AL, TL, JHe, TA, IK, JL; Software, ON, ONi, IF, AJ, OK, OKu, HV,
510 TV, JV, JT; Visualization, ON, ONi, IF, AJ, LM, PJ, OKu and comments from all; Writing – original draft preparation, all
511 authors; Writing – review & editing, all authors.

512 **10 Competing interests**

513 The authors declare that they have no conflict of interest.

514 **11 Acknowledgments**

515 The work of HAMK has been conducted within the research project: *Carbon 4.0 - Analysis and utilization of biological data*
516 *in complex carbon ecosystems* funded by the Ministry of Education and Culture of Finland [grant OKM/189/523/2018]. The
517 work by FMI was supported by Business Finland [grant 6905/31/2018], The Strategic Research Council at the Academy of
518 Finland [decision no 327214], the Academy of Finland Flagship Program [decision no 337552], the Ministry of Agriculture
519 and Forestry of Finland [grant VN/5094/2021] and Maj and Tor Nessling foundation (grant 202000391). The work by SYKE
520 was supported by The Strategic Research Council at the Academy of Finland [decision no 327350].

521

522 The authors want to thank the 20 farmers who allowed testing the framework on their Carbon Action fields. We also thank the
523 owner of Ruukki farm, Natural Resources Institute Finland (Luke), and their employees for making it possible to have a
524 measurement site there. In addition, we are thankful for the owners and staff of Qvidja farm.

525 **References**

526 Bauer, P., Thorpe, A., and Brunet, G.: The quiet revolution of numerical weather prediction, *Nature*, 525, 47–55,
527 <https://doi.org/10.1038/nature14956>, 2015.

528 Bellamy, P. H., Loveland, P. J., Bradley, R. I., Lark, R. M., and Kirk, G. J. D.: Carbon losses from all soils across England
529 and Wales 1978–2003, *Nature*, 437, 245–248, <https://doi.org/10.1038/nature04038>, 2005.

530 Bossio, D. A., Cook-Patton, S. C., Ellis, P. W., Fargione, J., Sanderman, J., Smith, P., Wood, S., Zomer, R. J., von Unger, M.,
531 Emmer, I. M., and Griscom, B. W.: The role of soil carbon in natural climate solutions, *Nat Sustain*, 3, 391–398,
532 <https://doi.org/10.1038/s41893-020-0491-z>, 2020.

533 Buizza, R. and Richardson, D.: 25 years of ensemble forecasting at ECMWF, <https://doi.org/10.21957/BV418O>, 2017.

534 Chang, W., Cheng, J., Allaire, J., Xie, Y., and McPherson, J.: Shiny: web application framework for R, 1, 2017, 2017.

535 Crowther, T. W., van den Hoogen, J., Wan, J., Mayes, M. A., Keiser, A. D., Mo, L., Averill, C., and Maynard, D. S.: The
536 global soil community and its influence on biogeochemistry, *Science*, 365, eaav0550, <https://doi.org/10.1126/science.aav0550>,
537 2019.

538 Dietze, M.: *Ecological Forecasting*, Princeton University Press, <https://doi.org/10.1515/9781400885459>, 2017.

539 Dietze, M. C., Fox, A., Beck-Johnson, L. M., Betancourt, J. L., Hooten, M. B., Jarnevich, C. S., Keitt, T. H., Kenney, M. A.,
540 Laney, C. M., Larsen, L. G., Loescher, H. W., Lunch, C. K., Pijanowski, B. C., Randerson, J. T., Read, E. K., Tredennick, A.
541 T., Vargas, R., Weathers, K. C., and White, E. P.: Iterative near-term ecological forecasting: Needs, opportunities, and
542 challenges, *Proc Natl Acad Sci USA*, 115, 1424–1432, <https://doi.org/10.1073/pnas.1710231115>, 2018.

543 Elmendorf, S. C., Jones, K. D., Cook, B. I., Diez, J. M., Enquist, C. A. F., Hufft, R. A., Jones, M. O., Mazer, S. J., Miller-
544 Rushing, A. J., Moore, D. J. P., Schwartz, M. D., and Weltzin, J. F.: The plant phenology monitoring design for The National
545 Ecological Observatory Network, *Ecosphere*, 7, e01303, <https://doi.org/10.1002/ecs2.1303>, 2016.

546 Fer, I., Kelly, R., Moorcroft, P. R., Richardson, A. D., Cowdery, E. M., and Dietze, M. C.: Linking big models to big data:
547 efficient ecosystem model calibration through Bayesian model emulation, *Biogeosciences*, 15, 5801–5830,
548 <https://doi.org/10.5194/bg-15-5801-2018>, 2018.

549 Fer, I., Gardella, A. K., Shiklomanov, A. N., Campbell, E. E., Cowdery, E. M., De Kauwe, M. G., Desai, A., Duveneck, M. J.,
550 Fisher, J. B., Haynes, K. D., Hoffman, F. M., Johnston, M. R., Kooper, R., LeBauer, D. S., Mantooth, J., Parton, W. J., Poulter,
551 B., Quaipe, T., Raiho, A., Schaefer, K., Serbin, S. P., Simkins, J., Wilcox, K. R., Viskari, T., and Dietze, M. C.: Beyond
552 ecosystem modeling: A roadmap to community cyberinfrastructure for ecological data-model integration, *Glob. Change Biol.*,
553 27, 13–26, <https://doi.org/10.1111/gcb.15409>, 2021.

554 Foken, Th. and Wichura, B.: Tools for quality assessment of surface-based flux measurements, *Agricultural and Forest*
555 *Meteorology*, 78, 83–105, [https://doi.org/10.1016/0168-1923\(95\)02248-1](https://doi.org/10.1016/0168-1923(95)02248-1), 1996.

556 Guerra, C. A., Bardgett, R. D., Caon, L., Crowther, T. W., Delgado-Baquerizo, M., Montanarella, L., Navarro, L. M., Orgiazzi,
557 A., Singh, B. K., Tedersoo, L., Vargas-Rojas, R., Briones, M. J. I., Buscot, F., Cameron, E. K., Cesarz, S., Chatzinotas, A.,
558 Cowan, D. A., Djukic, I., van den Hoogen, J., Lehmann, A., Maestre, F. T., Marín, C., Reitz, T., Rillig, M. C., Smith, L. C.,
559 de Vries, F. T., Weigelt, A., Wall, D. H., and Eisenhauer, N.: Tracking, targeting, and conserving soil biodiversity, *Science*,
560 371, 239–241, <https://doi.org/10.1126/science.abd7926>, 2021.

561 Heikkinen, J., Ketoja, E., Nuutinen, V., and Regina, K.: Declining trend of carbon in Finnish cropland soils in 1974–2009,
562 *Glob Change Biol*, 19, 1456–1469, <https://doi.org/10.1111/gcb.12137>, 2013.

563 Heikkinen, J., Keskinen, R., Regina, K., Honkanen, H., and Nuutinen, V.: Estimation of carbon stocks in boreal cropland soils
564 - methodological considerations, *Eur J Soil Sci*, 72, 934–945, <https://doi.org/10.1111/ejss.13033>, 2021.

565 Heimsch, L., Lohila, A., Tuovinen, J.-P., Vekuri, H., Heinonsalo, J., Nevalainen, O., Korhonen, M., Liski, J., Laurila, T.,
566 and Kulmala, L.: Carbon dioxide fluxes and carbon balance of an agricultural grassland in southern Finland, *Biogeosciences*,
567 18, 3467–3483, <https://doi.org/10.5194/bg-18-3467-2021>, 2021.

568 Hinckley, E. S., Bonan, G. B., Bowen, G. J., Colman, B. P., Duffy, P. A., Goodale, C. L., Houlton, B. Z., Marin-Spiotta, E.,
569 Ogle, K., Ollinger, S. V., Paul, E. A., Vitousek, P. M., Weathers, K. C., and Williams, D. G.: The soil and plant biogeochemistry
570 sampling design for The National Ecological Observatory Network, *Ecosphere*, 7, <https://doi.org/10.1002/ecs2.1234>, 2016.

571 Hipsey, M. R., Bruce, L. C., Boon, C., Busch, B., Carey, C. C., Hamilton, D. P., Hanson, P. C., Read, J. S., de Sousa, E.,
572 Weber, M., and Winslow, L. A.: A General Lake Model (GLM 3.0) for linking with high-frequency sensor data from the
573 Global Lake Ecological Observatory Network (GLEON), *Geosci. Model Dev.*, 12, 473–523, [https://doi.org/10.5194/gmd-12-](https://doi.org/10.5194/gmd-12-473-2019)
574 [473-2019](https://doi.org/10.5194/gmd-12-473-2019), 2019.

575 Höglind, M., Cameron, D., Persson, T., Huang, X., and van Oijen, M.: BASGRA_N: A model for grassland productivity,
576 quality and greenhouse gas balance, *Ecological Modelling*, 417, 108925, <https://doi.org/10.1016/j.ecolmodel.2019.108925>,
577 2020.

578 Huang, X., Zhao, G., Zorn, C., Tao, F., Ni, S., Zhang, W., Tu, T., and Höglind, M.: Grass modelling in data-limited areas by
579 incorporating MODIS data products, *Field Crops Research*, 271, 108250, <https://doi.org/10.1016/j.fcr.2021.108250>, 2021.

580 Keller, M., Schimel, D. S., Hargrove, W. W., and Hoffman, F. M.: A continental strategy for the National Ecological
581 Observatory Network, *Frontiers in Ecology and the Environment*, 6, 282–284, [https://doi.org/10.1890/1540-](https://doi.org/10.1890/1540-9295(2008)6[282:ACSFTN]2.0.CO;2)
582 [9295\(2008\)6\[282:ACSFTN\]2.0.CO;2](https://doi.org/10.1890/1540-9295(2008)6[282:ACSFTN]2.0.CO;2), 2008.

583 Knebl, L., Leithold, G., and Brock, C.: Improving minimum detectable differences in the assessment of soil organic matter
584 change in short-term field experiments, *J. Plant Nutr. Soil Sci.*, 178, 35–42, <https://doi.org/10.1002/jpln.201400409>, 2015.

585 Köchy, M., Hiederer, R., and Freibauer, A.: Global distribution of soil organic carbon – Part 1: Masses and frequency
586 distributions of SOC stocks for the tropics, permafrost regions, wetlands, and the world, *SOIL*, 1, 351–365,
587 <https://doi.org/10.5194/soil-1-351-2015>, 2015.

588 Lal, R., Negassa, W., and Lorenz, K.: Carbon sequestration in soil, *Current Opinion in Environmental Sustainability*, 15, 79–
589 86, <https://doi.org/10.1016/j.cosust.2015.09.002>, 2015.

590 Laurila, T., Tuovinen, J.-P., Lohila, A., Hatakka, J., Aurela, M., Thum, T., Pihlatie, M., Rinne, J., and Vesala, T.: Measuring
591 methane emissions from a landfill using a cost-effective micrometeorological method: MEASURING METHANE
592 EMISSIONS, *Geophys. Res. Lett.*, 32, n/a-n/a, <https://doi.org/10.1029/2005GL023462>, 2005.

593 Lloyd, J. and Taylor, J. A.: On the Temperature Dependence of Soil Respiration, *Functional Ecology*, 8, 315,
594 <https://doi.org/10.2307/2389824>, 1994.

595 Mattila, T.: Carbon action MULTA Finnish carbon sequestration experimental field dataset 2019,
596 <https://doi.org/10.5281/ZENODO.3670654>, 2020.

597 Mattila, T. J., Hagelberg, E., Söderlund, S., and Joona, J.: How farmers approach soil carbon sequestration? Lessons learned
598 from 105 carbon-farming plans, *Soil and Tillage Research*, 215, 105204, <https://doi.org/10.1016/j.still.2021.105204>, 2022.

599 Mattila, Tuomas and Heinonen, Reija: Carbon action MULTA Finnish carbon sequestration experimental field dataset 2020,
600 <https://doi.org/10.5281/ZENODO.4068271>, 2021.

601 McMillen, R. T.: An eddy correlation technique with extended applicability to non-simple terrain, *Boundary-Layer Meteorol*,
602 43, 231–245, <https://doi.org/10.1007/BF00128405>, 1988.

603 Meersmans, J., Van Wesemael, B., De Ridder, F., Fallas Dotti, M., De Baets, S., and Van Molle, M.: Changes in organic
604 carbon distribution with depth in agricultural soils in northern Belgium, 1960–2006: CHANGES IN SOC OF NORTHERN
605 BELGIUM, 15, 2739–2750, <https://doi.org/10.1111/j.1365-2486.2009.01855.x>, 2009.

606 Merante, P., Dibari, C., Ferrise, R., Sánchez, B., Iglesias, A., Lesschen, J. P., Kuikman, P., Yeluripati, J., Smith, P., and Bindi,
607 M.: Adopting soil organic carbon management practices in soils of varying quality: Implications and perspectives in Europe,
608 *Soil and Tillage Research*, 165, 95–106, <https://doi.org/10.1016/j.still.2016.08.001>, 2017.

609 Minasny, B., Malone, B. P., McBratney, A. B., Angers, D. A., Arrouays, D., Chambers, A., Chaplot, V., Chen, Z.-S., Cheng,
610 K., Das, B. S., Field, D. J., Gimona, A., Hedley, C. B., Hong, S. Y., Mandal, B., Marchant, B. P., Martin, M., McConkey, B.
611 G., Mulder, V. L., O'Rourke, S., Richer-de-Forges, A. C., Odeh, I., Padarian, J., Paustian, K., Pan, G., Poggio, L., Savin, I.,
612 Stolbovoy, V., Stockmann, U., Sulaeman, Y., Tsui, C.-C., Vågen, T.-G., van Wesemael, B., and Winowiecki, L.: Soil carbon
613 4 per mille, *Geoderma*, 292, 59–86, <https://doi.org/10.1016/j.geoderma.2017.01.002>, 2017.

614 Oldfield, E. E., Wood, S. A., and Bradford, M. A.: Direct effects of soil organic matter on productivity mirror those observed
615 with organic amendments, *Plant Soil*, 423, 363–373, <https://doi.org/10.1007/s11104-017-3513-5>, 2018.

616 Pastorello, G., Trotta, C., Canfora, E., Chu, H., Christianson, D., Cheah, Y.-W., Poindexter, C., Chen, J., Elbashandy, A.,
617 Humphrey, M., Isaac, P., Polidori, D., Reichstein, M., Ribeca, A., van Ingen, C., Vuichard, N., Zhang, L., Amiro, B., Ammann,
618 C., Arain, M. A., Ardö, J., Arkebauer, T., Arndt, S. K., Arriga, N., Aubinet, M., Aurela, M., Baldocchi, D., Barr, A.,
619 Beamesderfer, E., Marchesini, L. B., Bergeron, O., Beringer, J., Bernhofer, C., Berveiller, D., Billesbach, D., Black, T. A.,
620 Blanken, P. D., Bohrer, G., Boike, J., Bolstad, P. V., Bonal, D., Bonnefond, J.-M., Bowling, D. R., Bracho, R., Brodeur, J.,
621 Brümmer, C., Buchmann, N., Burban, B., Burns, S. P., Buysse, P., Cale, P., Cavagna, M., Cellier, P., Chen, S., Chini, I.,
622 Christensen, T. R., Cleverly, J., Collalti, A., Consalvo, C., Cook, B. D., Cook, D., Coursolle, C., Cremonese, E., Curtis, P. S.,
623 D'Andrea, E., da Rocha, H., Dai, X., Davis, K. J., Cinti, B. D., Grandcourt, A. de Ligne, A. D., De Oliveira, R. C., Delpierre,
624 N., Desai, A. R., Di Bella, C. M., Tommasi, P. di, Dolman, H., Domingo, F., Dong, G., Dore, S., Duce, P., Dufrêne, E., Dunn,
625 A., Dušek, J., Eamus, D., Eichelmann, U., ElKhidir, H. A. M., Eugster, W., Ewenz, C. M., Ewers, B., Famulari, D., Fares, S.,
626 Feigenwinter, I., Feitz, A., Fensholt, R., Filippa, G., Fischer, M., Frank, J., Galvagno, M., et al.: The FLUXNET2015 dataset

627 and the ONEFlux processing pipeline for eddy covariance data, *Scientific Data*, 7, 225, [https://doi.org/10.1038/s41597-020-](https://doi.org/10.1038/s41597-020-0534-3)
628 [0534-3](https://doi.org/10.1038/s41597-020-0534-3), 2020.

629 Qu, Z., Oumbe, A., Blanc, P., Espinar, B., Gesell, G., Gschwind, B., Klüser, L., Lefèvre, M., Saboret, L., Schroedter-
630 Homscheidt, M., and Wald, L.: Fast radiative transfer parameterisation for assessing the surface solar irradiance: The
631 Heliosat-4 method, *Meteorol Z*, 26, 33–57, <https://doi.org/10.1127/metz/2016/0781>, 2017.

632 Petchey, O. L., Pontarp, M., Massie, T. M., Kéfi, S., Ozgul, A., Weilenmann, M., Palamara, G. M., Altermatt, F., Matthews,
633 B., Levine, J. M., Childs, D. Z., McGill, B. J., Schaepman, M. E., Schmid, B., Spaak, P., Beckerman, A. P., Pennekamp, F.,
634 and Pearse, I. S.: The ecological forecast horizon, and examples of its uses and determinants, *Ecol Lett*, 18, 597–611,
635 <https://doi.org/10.1111/ele.12443>, 2015.

636 Rebmann, C., Kolle, O., Heinesch, B., Queck, R., Ibrom, A., and Aubinet, M.: Data Acquisition and Flux Calculations, in:
637 *Eddy Covariance*, edited by: Aubinet, M., Vesala, T., and Papale, D., Springer Netherlands, Dordrecht, 59–83,
638 https://doi.org/10.1007/978-94-007-2351-1_3, 2012.

639 Reichstein, M., Falge, E., Baldocchi, D., Papale, D., Aubinet, M., Berbigier, P., Bernhofer, C., Buchmann, N., Gilmanov, T.,
640 Granier, A., Grunwald, T., Havrankova, K., Ilvesniemi, H., Janous, D., Knohl, A., Laurila, T., Lohila, A., Loustau, D.,
641 Matteucci, G., Meyers, T., Miglietta, F., Ourcival, J.-M., Pumpanen, J., Rambal, S., Rotenberg, E., Sanz, M., Tenhunen, J.,
642 Seufert, G., Vaccari, F., Vesala, T., Yakir, D., and Valentini, R.: On the separation of net ecosystem exchange into assimilation
643 and ecosystem respiration: review and improved algorithm, *Global Change Biol*, 11, 1424–1439,
644 <https://doi.org/10.1111/j.1365-2486.2005.001002.x>, 2005.

645 Richardson, A. D., Mahecha, M. D., Falge, E., Kattge, J., Moffat, A. M., Papale, D., Reichstein, M., Stauch, V. J., Braswell,
646 B. H., Churkina, G., Kruijt, B., and Hollinger, D. Y.: Statistical properties of random CO₂ flux measurement uncertainty
647 inferred from model residuals, *Agricultural and Forest Meteorology*, 148, 38–50,
648 <https://doi.org/10.1016/j.agrformet.2007.09.001>, 2008.

649 Saby, N. P. A., Arrouays, D., Antoni, V., Lemerrier, B., Follain, S., Walter, C., and Schwartz, C.: Changes in soil organic
650 carbon in a mountainous French region, 1990-2004, 24, 254–262, <https://doi.org/10.1111/j.1475-2743.2008.00159.x>, 2008.

651 Sanderman, J., Hengl, T., and Fiske, G. J.: Soil carbon debt of 12,000 years of human land use, *Proc Natl Acad Sci USA*, 114,
652 9575–9580, <https://doi.org/10.1073/pnas.1706103114>, 2017.

653 Scharf, P. C., Shannon, D. K., Palm, H. L., Sudduth, K. A., Drummond, S. T., Kitchen, N. R., Mueller, L. J., Hubbard, V. C.,
654 and Oliveira, L. F.: Sensor-Based Nitrogen Applications Out-Performed Producer-Chosen Rates for Corn in On-Farm
655 Demonstrations, *Agron.j.*, 103, 1683–1691, <https://doi.org/10.2134/agronj2011.0164>, 2011.

- 656 Sela, S., Woodbury, P. B., and van Es, H. M.: Dynamic model-based N management reduces surplus nitrogen and improves
657 the environmental performance of corn production, *Environ. Res. Lett.*, 13, 054010, [https://doi.org/10.1088/1748-](https://doi.org/10.1088/1748-9326/aab908)
658 [9326/aab908](https://doi.org/10.1088/1748-9326/aab908), 2018.
- 659 Smith, P., Soussana, J., Angers, D., Schipper, L., Chenu, C., Rasse, D. P., Batjes, N. H., Egmond, F., McNeill, S., Kuhnert,
660 M., Arias-Navarro, C., Olesen, J. E., Chirinda, N., Fornara, D., Wollenberg, E., Álvaro-Fuentes, J., Sanz-Cobena, A., and
661 Klumpp, K.: How to measure, report and verify soil carbon change to realize the potential of soil carbon sequestration for
662 atmospheric greenhouse gas removal, *Glob Change Biol*, 26, 219–241, <https://doi.org/10.1111/gcb.14815>, 2020.
- 663 VandenBygaart, A. J. and Angers, D. A.: Towards accurate measurements of soil organic carbon stock change in
664 agroecosystems, *Can. J. Soil. Sci.*, 86, 465–471, <https://doi.org/10.4141/S05-106>, 2006.
- 665 Viskari, T., Laine, M., Kulmala, L., Mäkelä, J., Fer, I., and Liski, J.: Improving Yasso15 soil carbon model estimates with
666 ensemble adjustment Kalman filter state data assimilation, *Geosci. Model Dev.*, 13, 5959–5971, [https://doi.org/10.5194/gmd-](https://doi.org/10.5194/gmd-13-5959-2020)
667 [13-5959-2020](https://doi.org/10.5194/gmd-13-5959-2020), 2020.
- 668 Webb, E. K., Pearman, G. I., and Leuning, R.: Correction of flux measurements for density effects due to heat and water
669 vapour transfer, *Q.J Royal Met. Soc.*, 106, 85–100, <https://doi.org/10.1002/qj.49710644707>, 1980.
- 670 Weiss, M. and Baret, F.: S2toolbox Level 2 Products: Lai, Fapar, Fcover, 2016.
- 671 White, J. W., Hunt, L. A., Boote, K. J., Jones, J. W., Koo, J., Kim, S., Porter, C. H., Wilkens, P. W., and Hoogenboom, G.:
672 Integrated description of agricultural field experiments and production: The ICASA Version 2.0 data standards, *Computers*
673 *and Electronics in Agriculture*, 96, 1–12, <https://doi.org/10.1016/j.compag.2013.04.003>, 2013.